

Synthesis and Characterization of Epoxy-Acrylate Composite Latex

GUIRONG PAN, LIMIN WU, ZHUQING ZHANG, DAN LI

Department of Materials Science, Fudan University, Shanghai 200433, People's Republic of China

Received 22 January 2001; accepted 17 May 2001

ABSTRACT: A waterborne epoxy-acrylate composite latex was synthesized. The effects of the concentration of the initiator, surfactant, and epoxy resin on the particle size, molecular weight, and grafting ratios of the composite latex were investigated. The increase of the concentration of the initiator and epoxy resin led to the decrease of the weight-average molecular weight. The graft ratios increased with an increase in the initiator level and a decrease in the epoxy resin concentration whereas the variation of the concentration of the surfactant did not have much influence on the graft ratios. The increase in the initiator level caused the aggrandizement of the particle size, and the increase of the concentration of the surfactant and epoxy resin caused a decrease in the latex particle size. Fourier transform IR spectroscopy with attenuated total reflectance indicated that the epoxy resin molecules were enriched in the mold-facing surface in the film from the composite latex. The differential scanning calorimetry analysis, dynamic mechanical analysis, and Instron test showed that the polymer films cast by the composite latex had lower tensile strength and glass transition than those by the blend latex. © 2002 John Wiley & Sons, Inc. *J Appl Polym Sci* 83: 1736–1743, 2002

Key words: epoxy-acrylate composite latex; emulsion polymerization; dynamic mechanical analysis; Fourier transform IR spectroscopy with attenuated total reflectance

INTRODUCTION

Epoxy resins have been widely used as coatings, adhesives, and sealants because of their combined properties of toughness, flexibility, adhesion, and chemical resistance. However, in order to make them tractable, it is necessary to dilute the resins with organic solvents. Since the 1960s a substantial research effort has been made into the development of water-based epoxy systems because of the pressure to reduce volatile organic

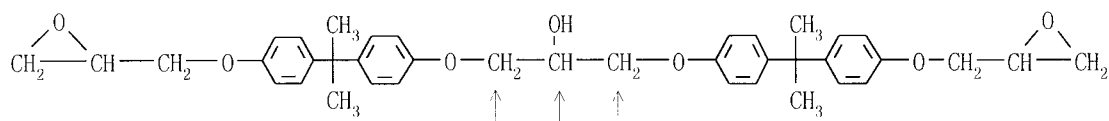
compounds, and some interesting methods have been proposed.^{1–4} One method is to produce water-based epoxy-acrylate copolymers via grafting polymerization.^{5–7}

Generally, the synthesis of a water-reducible epoxy-acrylate composite copolymer involves incorporating hydrophilic groups into the molecular chains of the epoxy resin to make it water dispersible. Water and organic solvents are used as cosolvents. Grafting along the epoxy backbone via hydrogen abstraction is usually used to introduce carboxyl groups. Abstraction of a hydrogen results in a free radical on the epoxy resin backbone, which serves as a grafting site for polymerization of acrylic monomers. The most probable grafting locations on epoxy resin molecular chains are indicated by the arrows in the following⁸:

Correspondence to: L. Wu (lxw@fudan.ac.cn).

Contract grant sponsor: National Nature and Science Foundation of China; contract grant number: 59873004.

Journal of Applied Polymer Science, Vol. 83, 1736–1743 (2002)
© 2002 John Wiley & Sons, Inc.
DOI 10.1002/app.10100



Thus, for each unit $\text{—O—CH}_2\text{—}\overset{\text{OH}}{\text{C}}\text{—CH}_2\text{—O—}$, there are five hydrogen atoms that can be abstracted by free radicals to form grafting sites where acrylic monomers containing acrylic acid (AA) or methacrylic acid are initiated and polymerized. Although the hydrogen atom at the tertiary carbon is more easily abstracted than at the secondary carbon, the grafting ratio at the secondary carbon is probably much higher than at the tertiary carbon because of more hydrogen atoms at the secondary carbon. The copolymer containing a carboxylic group is finally neutralized with an amine such as dimethylaminoethanol and diluted with water to obtain water-borne systems.^{9–11} Woo and Toman^{8,9} synthesized the water-reducible epoxy-acrylic composite copolymers based on the above principle. A ¹³C-NMR spectroscopy analysis showed that the grafting ratio at the secondary carbon ($\text{—CH}_2\text{—}$) to that at the tertiary carbon (—CH—) is 2.7:1. Egusa et al.^{6,7} conducted electron-beam irradiation of highly viscous systems of epoxy resin dissolved in monomer mixtures of acrylic monomers and styrene (St) with *n*-butanol, cyclohexanone, and water as cosolvents to obtain a water-based epoxy-acrylic composite system.

In this study the epoxy-acrylic composite latex was synthesized using emulsion polymerization, which completely eliminated the organic solvents employed in the water-reducible epoxy-acrylic copolymer. The effects of the concentration of the initiator, surfactant, and epoxy resin on the molecular weight, graft ratio, and particle size of the composite latex were investigated. Fourier transform IR spectrometry with attenuated total reflectance (FTIR-ATR), differential scanning calorimetry (DSC), dynamic mechanical analysis (DMA), and an Instron tensile machine were used to analyze the structure and properties of the obtained composite and blend latex.

EXPERIMENTAL

Materials

Butyl acrylate (BA, 96%), St (97%), and AA (98%) were purchased from Shanghai Gaoqiao Petro-

chemical Company. The epoxy resin (0.38–0.45 epoxy value) was kindly provided by Shanghai Resin Company. The anionic surfactant polyoxyethylene alkylphenyl ether ammonium sulfate (Phodapex CO436, 4 mol ethylene oxide) and the nonionic surfactant polyoxyethylene octylphenyl ether (Igepal CA897, 40 mol ethylene oxide) were supplied by Rhone-Poulenc. Ammonium persulfate and sodium bicarbonate were purchased from Shanghai Chemistry Reagent Company. All materials were used without further purification.

Preparation of Composite Latex

The synthesis of composite latex was carried out in a 500-mL four-necked round-bottom flask equipped with a mechanical stirrer, addition funnel, N₂ inlet, thermometer, and heating mantle. The epoxy resin, emulsifier, part of the acrylic monomers, and water as indicated in Table I (Part A) were preemulsified and added to the flask at 60°C and stirred and heated to 70°C for 1 h to obtain the seed latex. This was followed by the addition of the preemulsified monomer mixture and the mixture of the initiator and buffer solution as indicated in Table I (Part B) over a period of 2 h using an addition funnel and a constant flow pump, respectively, at 70°C under a stream of N₂. After adding all the ingredients, the reaction mixture was heated for an additional 1.5 h to complete the reaction of the residual

Table I Typical Recipe for Synthesis of Epoxy-Acrylic Composite Latex

| Materials | Part A (g) | Part B (g) |
|--|---------------|---------------|
| Epoxy resin | 20 | 0 |
| BA | 5 | 35 |
| St | 5 | 35 |
| AA | 2 | 0 |
| PAA | 2 | 0 |
| Surfactants (CO436 + CA897) | 6 | 1 |
| Buffer (NaHCO ₃) | 0.5 | 1 |
| Initiator [(NH ₄) ₂ S ₂ O ₈] | 1 | 1 |
| Deionized H ₂ O | 70 | 80 |

monomers to obtain the composite latex, which is composed of ungrafted epoxy, epoxy-acrylate graft copolymer, and ungrafted acrylic copolymer. The degree of the conversion is around 99%.

Preparation of Latex Blend

The epoxy resin combined with anionic and non-ionic surfactants were charged into a flask and dispersed at high speed at 70–80°C. The deionized water preheated to 80°C was slowly added into the flask during the dispersion to yield a water in oil solution. When 10–20% water was added, the solution began to invert into an oil in water solution. When 40–60% of the addition was completed, the phase conversion was finished. The epoxy solution with a solid content of 40% was finally obtained.¹² The St-BA copolymer latex was synthesized in the same polymerization condition described for graft polymerization. Then the epoxy emulsion and the St-BA copolymer latex were mixed to obtain a physical blend latex with the same weight ratio of epoxy resin to St-BA copolymer as in the composite latex.

Sample Characterization

The composite latex was demulsified with methanol, washed 5 times with deionized water, followed by drying at 50°C under a vacuum oven for 24 h to obtain the composite copolymers. The molecular weight, molecular weight distribution, and the graft ratio were obtained by running 0.5 wt % composite copolymer in tetrahydrofuran (THF) through a Waters liquid chromatograph at 30°C. This system consisted of a Waters 150 pump, a detector for the refractive index (RI), and UV and two Ultrastaygel columns. THF was used as the eluent phase. The elution volumes were converted to apparent molecular weights using narrow distribution polystyrene standards.

The particle size of the composite latex was obtained from the measurement with a Coulter LS230 particle size analyzer (Coulter, Miami, FL), which has a measurement range of 0.04–2000 μm .

The FTIR-ATR spectra were obtained using a ZnSe internal reflectance element at an incidence angle of 45° with a HATR ATR accessory that was placed in the sample compartment of a Magna-IR 550 FTIR spectrometer (Nicolet Instruments, Madison, WI). The scanning was repeated at least 200 times before the spectra were recorded at a resolution of 2 cm^{-1} . The composite latex was cast

on clean glass and dried to prepare the films for FTIR-ATR analysis.

The polymer latexes were demulsified, washed, dried, and then analyzed by a DSC calorimeter (Dupont DSC 10) for the thermal behavior analysis. The DSC scanning was performed from –100 to 100°C at a heating rate of 10°C/min under a nitrogen atmosphere.

Dynamic mechanical measurements were carried out on DMA 242 (Netzsch Inc.). The samples were quickly cooled to –50°C and equilibrated at that temperature for 3 min, then heated to 120°C at a frequency of 0.1 Hz with a constant heating rate of 5°C/min under a nitrogen atmosphere. The samples for DMA were cut from the polymer films that were prepared by casting the latex on the glass and drying at 50°C for 1 week.

An Instron model DXLL 1000–20,000 testing machine (Shanghai, China) was employed for the tensile tests. The dumbbell-shaped specimens for the tensile tests were cut from sample films that were prepared by casting the latex on glass and drying at 50°C for 1 week. The tests were carried out at a crosshead speed of 500 mm/min according to Die C of ASTM D412. A 25-mm benchmark and the original cross-sectional area were utilized to calculate their tensile properties. The ultimate tensile strength and elongation were automatically calculated by the computer connected to the Instron. The average of at least five measurements for each sample was reported, and the experimental error is $\pm 10\%$.

RESULTS AND DISCUSSION

Molecular Weight, Grafting Ratio, and Particle Size of Composite Latex

Figures 1 and 2 are typical representatives of the gel permeation chromatography (GPC) measurements for the composite copolymers using the RI detector and UV detector, respectively. In the RI curve the first peak corresponds to a molecular weight of more than 100,000, which can be taken as the GPC chromatogram of the copolymer, including the epoxy-acrylic graft copolymer and the ungrafted acrylic copolymer. The second one corresponds to a molecular weight of less than 1000, which is obviously the GPC chromatogram of the ungrafted epoxy resin. Table II summarizes the number-average (M_n) and weight-average (M_w) molecular weights and polydispersity (M_w/M_n) for all composite copolymers. The weight-average

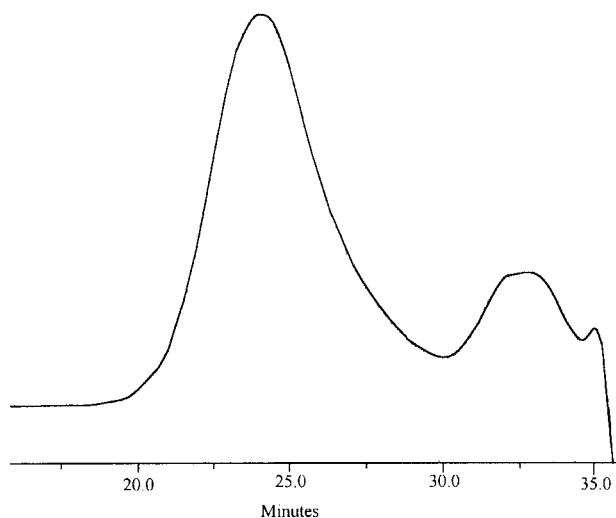


Figure 1 A gel permeation chromatogram of the composite copolymer by the refractive index detector.

molecular weight is reduced with the increase of the initiator concentration, which is consistent with traditional emulsion polymerization theory.¹³ The increase in the epoxy resin concentration corresponds to the decrease in the acrylic monomer concentration, so the weight-average molecular weight decreases. The number-average molecular weight does not have an obvious change because it is only sensitive to those species with small molecular weight and is dominated by epoxy resin molecules. The variation of the concentration of the surfactant does not have much influence on the molecular weight.

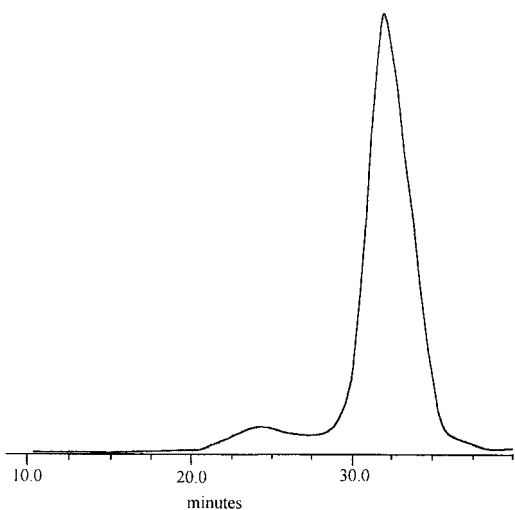


Figure 2 A gel permeation chromatogram of the composite copolymer by the UV detector.

Table II Molecular Weight of Epoxy-Acrylic Graft Copolymer

| Parameters | Concn Variation (wt %) ^a | M_w | M_n | M_w/M_n |
|-------------------|-------------------------------------|--------|-------|-----------|
| Initiator concn | 0.25 | 170000 | 71000 | 2.39 |
| | 0.5 | 130000 | 44000 | 2.95 |
| | 1.0 | 120000 | 45000 | 2.67 |
| | 1.25 | 110000 | 45000 | 2.44 |
| Surfactant concn | 3 | 120000 | 46000 | 2.61 |
| | 4.5 | 110000 | 48000 | 2.29 |
| | 6 | 120000 | 45000 | 2.67 |
| | 9 | 120000 | 49000 | 2.45 |
| Epoxy resin concn | 0 | 200000 | 44000 | 4.54 |
| | 5 | 160000 | 49000 | 3.27 |
| | 10 | 150000 | 50000 | 3.00 |
| | 15 | 140000 | 54000 | 2.59 |
| | 20 | 90000 | 41000 | 2.20 |

^a Based on the total masses of epoxy resin and acrylic monomers.

In the UV curve only the epoxy parts in the composite copolymers, including the ungrafted epoxy resin and the epoxy-acrylic graft copolymer, can be detected when the UV detector was set at 284 nm, which is based on the fact that the epoxy resin has a strong absorption at this wavelength due to the bisphenol A structure while the acrylic copolymer is almost transparent. Thus, the peak with low retention time is the GPC chromatogram of the epoxy-acrylic graft copolymer and the peak with high retention time is the GPC chromatogram of the ungrafted epoxy resin in the UV curve. Therefore, the graft ratios can be calculated using the ratio of the peak area of the epoxy-acrylic graft copolymer to the sum of the peak areas of the epoxy-acrylic graft copolymer and ungrafted epoxy resin in the UV curve based on Egusa et al.,⁶ as indicated in Table III. The values of the peak areas could be read directly from the data report calculated by the computer connected to the machine. The results show an increase in the graft ratio as the initiator level increases; this is because the increase in the initiator level results in an increase in the concentration of free radicals, increasing the probability of catching hydrogen atoms on the epoxy resin molecules; that is, this aggrandizes the probability of graft polymerization. The increase in the epoxy resin concentration causes an increase in the numbers of active hydrogen atoms, but the increase in the epoxy resin concentration de-

Table III Graft Ratio of Epoxy-Acrylic Graft Copolymer

| Initiator Concn (wt %) | Graft Ratio (%) | Surfactant Concn (wt %) | Graft Ratio (%) | Epoxy Resin Concn (wt %) | Graft Ratio (%) |
|---------------------------|--------------------|----------------------------|--------------------|-----------------------------|--------------------|
| 0.25 | 1.13 | 3 | 3.87 | 5 | 6.38 |
| 0.75 | 1.92 | 6 | 2.53 | 10 | 5.34 |
| 1.0 | 2.53 | 7.5 | 3.84 | 15 | 3.46 |
| 1.25 | 3.39 | 9 | 3.86 | 20 | 2.53 |

creases the concentration of acrylic monomers concurrently because the total solid content was maintained constant in our experiments. As a result, graft branches decrease; in other words, the graft ratio has a decreasing trend with the augmentation of the epoxy resin concentration. The variation in the surfactant concentration has little influence on the graft ratios.

Table IV assembles the effects of the concentrations of the initiator, surfactant, and epoxy resin on the particle size of the composite latex. The experimental results indicate an increasing trend in particle size with the increase of the initiator level, which is different from the traditional emulsion polymerization theory wherein the increase of the initiator level should cause the decrease of the particle size.¹³ The reason why the average particle size increases with the increase in the initiator level is not quite clear at present; it might be speculated that the increase in the initiator concentration leads to an increase in the probability of graft polymerization of acrylic monomers onto epoxy resin backbones, making more acrylic monomers enter into seed latex particles, resulting in an increasing trend in the average particle size. When the surfactant concentration increases, the particle size has a decreasing trend, which is attributed to the aggrandizement of the numbers of micelles, which increases the number of latex particles and decreases the average latex particle size. The in-

crease of the epoxy resin concentration causes an increasing trend in the latex particle size; this is possibly because the epoxy resin was postemulsified, which usually generates a slightly larger particle size than that from emulsion polymerization.

Structure and Properties of Epoxy-Acrylic Composite Latex and Blend Latex

The composite latex with different levels of epoxy resin were cast on clean glass and dried to prepare the films for FTIR and FTIR-ATR analyses. Figure 3 demonstrates the representative spectra for the air-facing side, mold-facing side and bulk of the composite copolymer containing 20 wt % epoxy resin. The three spectra display similar absorbing bands at the same wavelength, suggesting that they are analogous in structure. If the peak at 1508 cm^{-1} for stretching of *para*-phenyl could be indicated as the concentration for the epoxy resin and the peak at 1729 cm^{-1} for the absorption of carbonyl used as an index for the concentration of the acrylic-St copolymer,¹⁴ then the relative concentration of the epoxy distributed in the film can be judged by the absorbance ratio of the peak area at 1508 cm^{-1} to the peak area at 1729 cm^{-1} (A_{1508}/A_{1729}), as shown in Table V. The A_{1508}/A_{1729} ratios at the mold-facing side are higher than those at the air-facing side and bulk, suggesting that the epoxy resin part in the com-

Table IV Particle Size for Epoxy-Acrylic Composite Latex

| Initiator Concn (wt %) | Ave. Particle Diameter (μm) | Surfactant Concn (wt %) | Ave. Particle Diameter (μm) | Epoxy Resin Concn (wt %) | Ave. Particle Diameter (μm) |
|---------------------------|---|----------------------------|---|-----------------------------|---|
| 0.25 | 0.112 | 3 | 0.128 | 0 | 0.118 |
| 0.5 | 0.117 | 4.5 | 0.127 | 5 | 0.123 |
| 1.0 | 0.125 | 6 | 0.125 | 10 | 0.120 |
| 1.25 | 0.123 | 7.5 | 0.121 | 15 | 0.123 |
| | | 9 | 0.0818 | 20 | 0.125 |

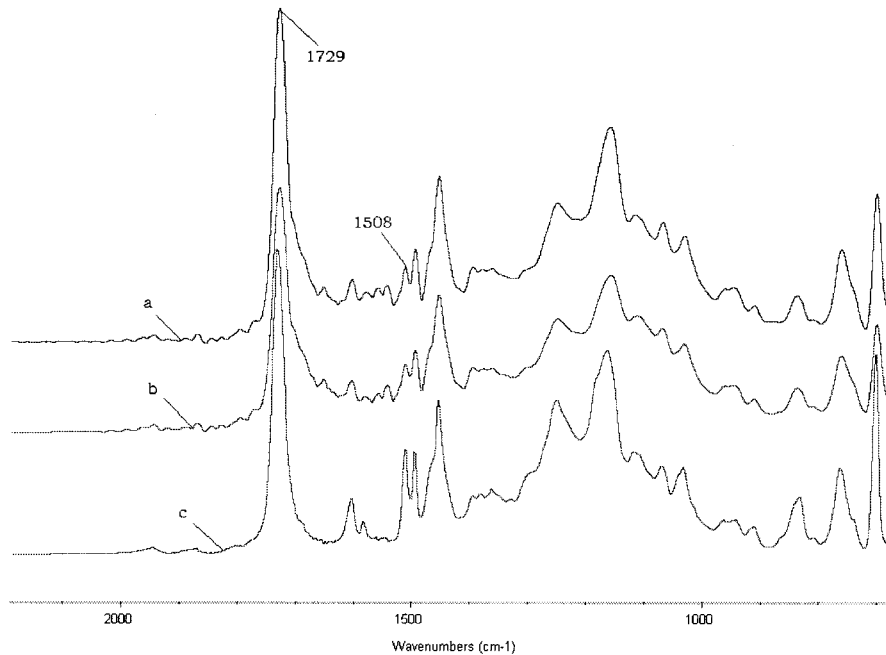


Figure 3 The FTIR-ATR spectra of the composite copolymer (a) mold-facing surface, (b) air-facing surface, and (c) bulk.

posite copolymer tends to move to the mold-facing side. The driving force for this movement could be attributed to the difference in the surface free energy between the epoxy resin and the acrylic-St copolymer. The critical surface tensions of the poly(BA) and polystyrene are around 31 and 33 mN/m, respectively, so the critical surface tension of the acrylic-St copolymer should be between 31 and 33 mN/m, which is lower than that of the epoxy resin, which is around 44 mN/m.^{15,16} Thus, during the process of casting and drying the composite films, the acrylic-St copolymer segments tried to segregate near the air-facing layer and the epoxy segments moved to the mold-facing side to minimize the surface energy. This migration is very beneficial in the application of coatings, adhesives, and electron sealants because epoxy res-

ins have excellent adhesion to substrates while acrylic copolymers remaining on the air-facing side have very good weatherability and appearance.

The DSC measurements as indicated in Figure 4 show two relaxation transitions at around 17.7 and 60°C for the blend polymer, two relaxation transitions at around 18.7 and 42.2°C for the com-

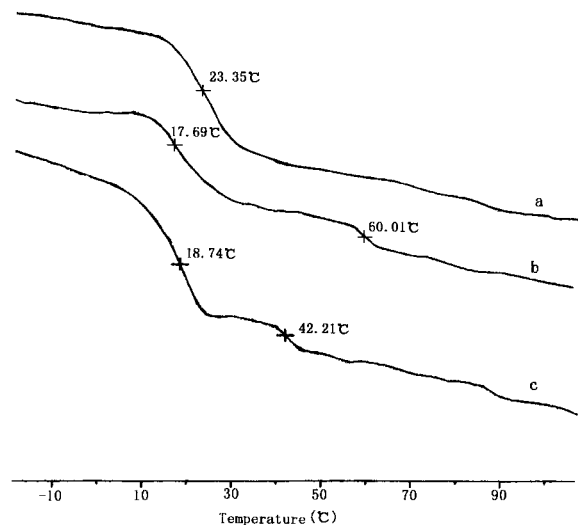


Figure 4 The DSC curves of (a) acrylic-styrene copolymer, (b) blend polymers, and (c) composite copolymer.

Table V Analysis Results of FTIR-AIR

| Epoxy Resin Concn (wt %) | A_{1508}/A_{1729} | | |
|--------------------------------|---------------------|-----------|-------|
| | Air Side | Mold Side | Bulk |
| 5 | 0.348 | 0.395 | 0.360 |
| 10 | 0.289 | 0.315 | 0.302 |
| 15 | 0.311 | 0.346 | 0.329 |
| 20 | 0.442 | 0.562 | 0.492 |

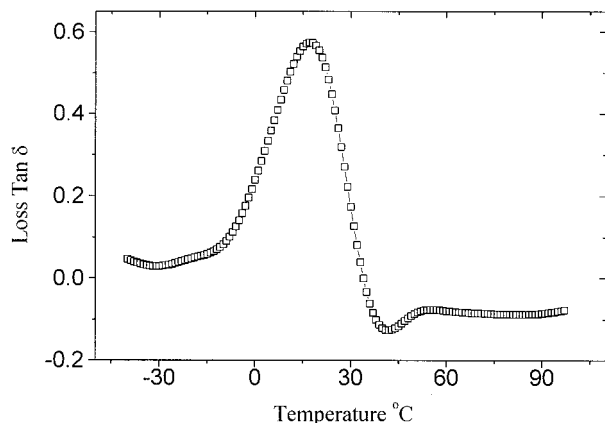


Figure 5 The loss $\tan \delta$ of the film from the blend latex as a function of the temperature.

posite copolymer, and one transition at around 23°C for the pure acrylic-St copolymer. The transitions at low temperature should come from micro-Brownian segmental motion of the amorphous acrylic-St copolymer because it is very close to the glass transition of the pure acrylic-St copolymer. The glass transitions of the acrylic-St copolymer from the composite latex and blend latex are lower than that of the pure acrylic-St copolymer because the epoxy resin has the function of being a plasticizer, which has no glass transition observed by DSC due to its low molecular weight. The DMA as demonstrated in Figures 5 and 6 further confirms the DSC results, also indicating two relaxation transitions at around 17.2 and 55.5°C for the blend polymer and two at around 15.4 and 48°C for the composite copolymer, respectively. Again, the transitions at low temperature should be from the micro-Brownian seg-

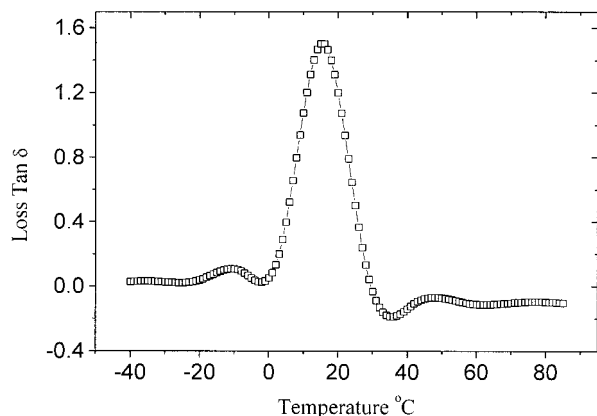


Figure 6 The loss $\tan \delta$ of the film from the composite latex as a function of the temperature.

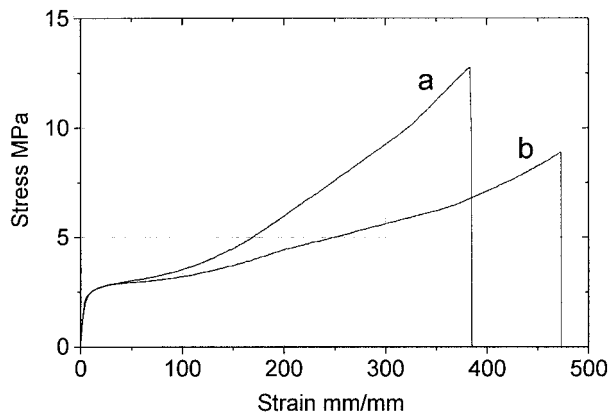


Figure 7 The stress-strain curves of the (a) latex blend film and (b) composite latex film.

mental motion of the amorphous acrylic-St copolymer. This transition at high temperature is interesting, which took place at around 42–60°C, as indicated by DSC and DMA curves for the blend polymer and composite copolymer. Obviously, this transition is not from the micro-Brownian segmental motion of the amorphous epoxy-acrylic graft copolymer because the blend polymer also has it, and this transition from the blend polymer occurred at higher temperature than that from the composite copolymer. This means that some reaction such as a crosslinking reaction between the epoxy resin and acrylic-St copolymer had happened and the blend polymer seemed to have a higher degree of crosslinking than the composite copolymer, which is further confirmed by gel experiments at 42.3 and 35.1% for the blend latex and composite latex, respectively. In addition, a small transition appears at -10.6°C on the DMA curve of the composite copolymer that is not observed on the DMA curve of the blend polymer; this transition is probably a π transition connected to the small-scale motion of the acrylic-St segmental chains grafting on the epoxy backbone.¹⁷ Woo and Toman also demonstrate the presence of graft copolymer using ^{13}C -NMR.⁹

The films made by casting a blend latex and composite latex on clean glass and drying at room temperature for 1 week were conducted on an Instron tensile machine. Figure 7 demonstrates their stress-strain curves; the blend copolymer has much higher tensile strength than the composite copolymer, being around 12.0 and 3.6 MPa, respectively, which further gives a hint that the blend polymer has higher crosslink density than the composite copolymer. The reason why the

blend polymer has higher crosslink density than the composite copolymer is under further investigation.

CONCLUSION

A waterborne epoxy-acrylic composite latex was synthesized. The increase of the initiator and epoxy resin concentrations led to a decrease in the weight-average molecular weight. The graft ratio increased with the enhancement of the initiator level and the reduction of epoxy resin concentration. The variation in the surfactant concentration did not have much influence on the weight-average molecular weight and graft ratio. The increase in the initiator level caused the aggrandizement of the particle size, and the increase of the surfactant and epoxy resin decreased the latex particle size.

The epoxy segments in the film of the composite latex had a trend to move to the mold-facing surface whereas the acrylic-St copolymer component segregated near the air-facing surface. The DSC measurements, DMA, tensile tests, and gel experiment showed that the blend polymer seemed to have higher crosslink density than the composite copolymer.

The authors would like to thank the National Nature and Science Foundation of China for the financial support of this project.

REFERENCES

1. Dante, M. F.; Allen, R. A. U.S. Pat. 4,316,003, 1982.
2. Shih, Y. J. U.S. Pat. 5,981,627, 1999.
3. Hare, C. H. *Mod Paint Coat* 1996, February, 23.
4. de Wet-Roos, D.; Knoetze, J. H.; Cooray, B.; Sanderson, R. D. *J Appl Polym Sci* 1999, 71, 1347.
5. Evans, J.; Ting, I.; Vincent, W. U.S. Pat. 4,212,781, 1980.
6. Egusa, S.; Sasaki, T.; Hagiwara, M. *J Appl Polym Sci* 1987, 34, 2163.
7. Egusa, S.; Sasaki, T.; Hagiwara, M. *J Appl Polym Sci* 1987, 34, 2177.
8. Woo, J. T. K.; Toman, A. *Progr Org Coat* 1993, 21, 371.
9. Woo, J. T. K.; Toman, A. *J Coat Technol* 1982, 54, 41.
10. Robinson, P. V. *J Coat Technol* 1981, 53, 23.
11. Wicks, Z. W.; Jones, F. N.; Pappas, S. P. *Organic Coatings Science and Technology*, 2nd ed.; Wiley: New York, 1998.
12. Wu, L.; Pan, G.; Zhang, Z. *Chin. Pat.* 1257881A, 2000.
13. Piirma, I. *Emulsion Polymerization*; Academic: New York, 1982.
14. Wang, Z. *The Infrared Spectra of Polymers*; Sichun University Press: Chengdu, 1989.
15. Wu, S. In *Polymer Blends*; Paul, D. R., Newman, S., Eds.; Academic: New York, 1978; Vol. 1.
16. Shafrin, E. G. In *Polymer Handbook*, 2nd ed.; Brandrup, J., Immergut, E. H., Eds.; Wiley-Interscience: New York, 1975.
17. He, M.; Chen, W.; Dong, X. *Polymer Physics*; Fudan University Press: Shanghai, 1990.